Efagins – engineerable agents that evolved independently to target the enterococcal cell wall

Janira Prichula,[1,2,3] Abigail L. Manson,[3] Joshua T. Smith,[3] Natia Karumidze,[4,5] Gracie Richards,[3] Suelen S. Mello,[1,2] Artur Czajkowski,[6] Mohammed Kaplan,[6] Ashlee M. Earl,[3]* and Michael S. Gilmore,[1,2,3]*

[1]Department of Ophthalmology, Massachusetts Eye and Ear Infirmary, Harvard Medical School, Boston, MA, USA

[2]Department of Microbiology, Harvard Medical School, Boston, MA, USA

[3]Infectious Disease and Microbiome Program, Broad Institute of MIT and Harvard, Cambridge, MA, USA

[4]Eliava Institute of Bacteriophages, Tbilisi, Georgia

[5]European University, Tbilisi, Georgia

[6]University of Chicago, Chicago, IL, USA

***Co-corresponding authors:** aearl@broadinstitute.org (A.M.E.) and michael_gilmore@meei.harvard.edu (M.S.G.)

ABSTRACT

Enterococci are major causes of multidrug-resistant infections, and antimicrobials with fundamentally new mechanisms of action are urgently needed. We identify a new class of antibacterial agents, termed efagins, which are chromosomally encoded, phage-related nanomachines that recognize cell wall carbohydrate receptors and inhibit subsets of *E. faecalis, E. faecium* and other enterococci selectively—a key reason they evaded prior detection. Five natural variants with distinct targeting profiles were identified – four related by sequence divergence, while one appears to have arisen through recombination of the targeting domain, likely from a phage donor. Operons encoding the corresponding carbohydrate receptors are highly variable, accounting for targeting specificity. The efagin targeting domain can be engineered to reprogram them toward alternative receptors, providing a pathway for filling critical coverage gaps. These findings advance

efagins as new selective antibacterials with promise for addressing infection and spread of multidrug-resistant enterococcal infection.

KEYWORDS

Enterococcus faecalis; generalist species, efagin, phage-related elements; antimicrobial agents; Epa; Rha-CWPS; VRE; *Enterococcus faecium*; hospital acquired infection

INTRODUCTION

Enterococci are projected to have evolved as gut microbes of land animals about the time arthropods first terrestrialized 400 – 500 MYA,[1] but now rank among leading causes of multidrug-resistant (MDR) infections of humans worldwide.[2–4] Of over 90 species present in diverse land animals[5], two that are distantly related[1] – *E. faecalis* and *E. faecium* – cause the vast majority of MDR human infection. Because of their ancient origins both naturally occur in non-human hosts, with *E. faecalis* being by far the greatest generalist of all enterococci.[5] This raised the question as to what unique features of *E. faecalis* distinguish it from all other enterococcal species and allow it to successfully compete with more specialized enterococci and other species, and colonize diverse gut consortia as they are conveyed up and down the food chain.

Comparing >3,000 *E. faecalis* genomes from diverse ecologies, we observed that despite its ancient emergence and host diversification over eons, a 14.6 kb cluster of genes previously annotated as encoding a partial phage[6] (which could not be ascribed phage function even in the presence of helper phages[7]) was highly conserved in all strains with reading frames well maintained. We interpret this as evidence that the product of this block of genes contributes fundamentally to the biology of *E. faecalis* in the highly diverse ecosystems in which it occurs.

Here, we show that this gene block encodes an independently evolved entity with antimicrobial activity that targets the rhamnose-rich enterococcal cell wall polysaccharide (Rha-CWPS) of enterococci and possibly

other microbes. We term its product efagin (*E. faecalis* phage-related inhibitor). Although sharing little sequence identity, efagins appear organizationally related to independently derived elements termed tailocins.[8,9] Efagin activity extends beyond *E. faecalis* to include many *E. faecium* and other enterococci, likely contributing to the success of this species in colonizing diverse animal guts. The efagin targeting domain is amenable to reprogramming through domain swaps, highlighting a pathway for filling critical gaps in coverage and potentially targeting new organisms.

RESULTS

Efagins are encoded within all *E. faecalis* genomes from diverse ecosystems and are exclusive to the species.

In a comparison of 3,068 genome sequences from diverse geographic and ecological sources, the efagin operon was found to be very highly conserved (Fig. 1, Table S1). All high-quality drafts (fewer than 75 contigs, n=2278) possess the entire element with reading frames intact; only five publicly available, low-quality draft genomes the lacked the full element did have partial hits. No *E. faecalis* genomes were found lacking efagin genes. The efagin gene cluster shows no evidence of mobility as its chromosomal neighborhood is highly conserved discounting any association with a mobile element (Extended Data Fig. 1). Efagin is therefore core to the *E. faecalis* species, and we interpret the high level of sequence conservation to reflect strong selection in diverse ecosystems.

To determine if efagin or anything analogous occurs in other enterococcal species, we searched a dataset of 15,854 *Enterococcaceae* genomes not including *E. faecalis*. No significant identity to efagin (>90% coverage; E-value <10) was found. A search of all draft prokaryotic genomes (approximately 1.2 million submissions) in NCBI (https://www.ncbi.nlm.nih.gov) similarly did not identify significant identities outside of *E. faecalis*. A broader search for: i) the presence of at least a partial phage, and ii) its occurrence in at least 50% of strains of a species (using the Genomad provirus detection tool[10] with candidate prophage protein annotations confirmed using Phastest[11]) found that *E. faecalis* efagin was the

74 only example fitting those criteria. Our search did identify an unrelated incomplete *Melissococcus*
75 *plutonius* prophage present in 89.5% of the comparatively few genomes available for that species (17/19;
76 Tables S2 and S3). However, its structural characteristics diverge from those of efagin as the *M. plutonius*
77 element is predicted to encode a capsid and scaffold proteins suggestive of a defective phage or gene
78 transfer agent[12] (Table S3), in contrast to efagins, which are characterized by a complete absence of phage
79 head-related genes (Fig. 1a; Extended Data Fig.2; Supplementary Fig. 1).

80 **Efagins are evolutionarily distant from Gram-positive and Gram-negative phage-related**
81 **antimicrobial agents**

82 Other antimicrobial phage-related systems have been identified.[13–24] Though efagin shares little to no
83 sequence identity with any, its genetic organization is broadly similar to the tailocin, monocin[20–22]
84 (Extended Data Fig. 2). At the amino acid sequence level, evidence of distant sequence identity is
85 detectable only between three protein counterparts (putative regulatory element EF1276 exhibits 40%
86 amino acid identity over 90% of its length with a monocin counterpart, whereas putative structural
87 components EF1288 and EF1292 exhibit 21% identity over 59% of length, and 38% over 49% of the
88 length respectively [Table S4]). For comparison, the ubiquity of monocin and other tailocins within
89 genomes of the respective species that express them was examined and found to vary widely in contrast to
90 the high degree of efagin conservation in *E. faecalis* (Tables S5-12; Extended Data Fig. 3). In current
91 databases, *E. faecalis* phage vB_EfaS_IME197 (41.3 kb)[25] exhibits the closest relationship – six efagin
92 proteins share 24.6% to 70.7% amino acid sequence identity with its inferred gene products (Table S13),
93 highlighting its independent evolution.

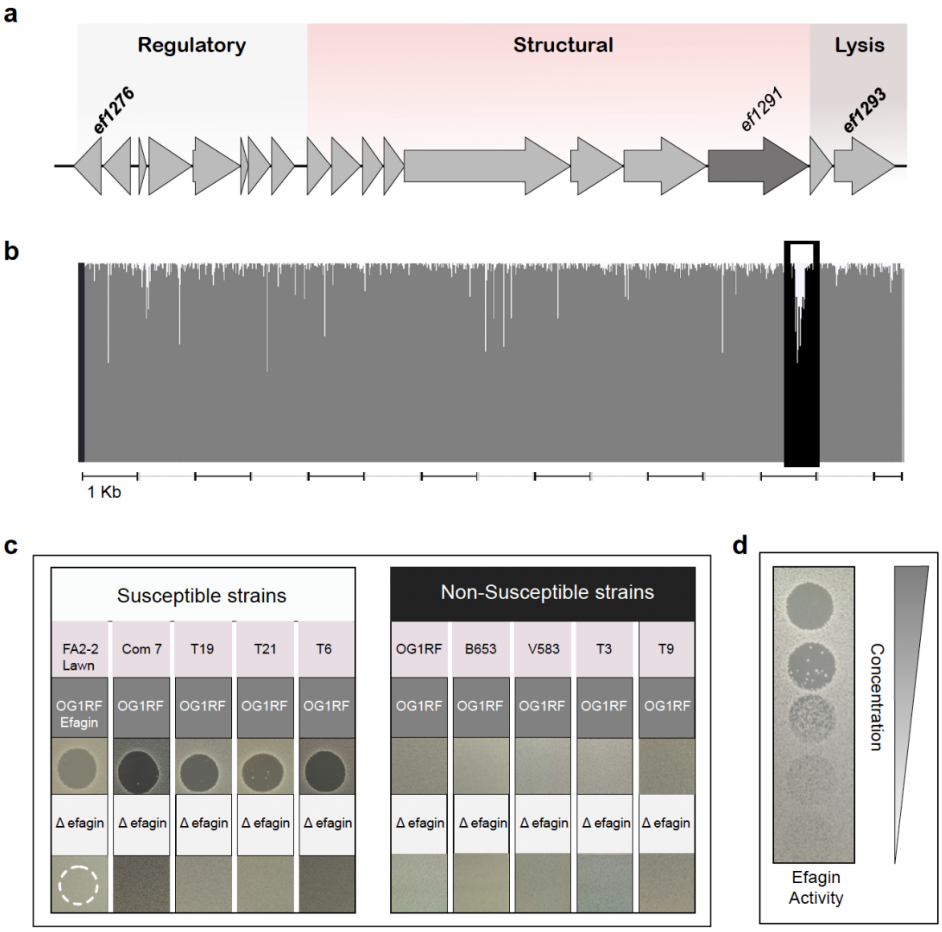

Fig 1. Efagin is core to *E. faecalis* and highly conserved except for a discrete variable region. a, Genetic organization of the 14.6kb efagin gene cluster, which in strain V583 consists of genes *ef1276 – ef1293*. **b,** Alignment of corresponding sequences in 2,774 high quality *E. faecalis* genomes using MUSCLE[26] shows the largest cluster of variability to occur in the C-terminal domain-encoding sequence of *ef1291* (highlighted). **c,** Efagin inhibits growth of select heterologous *E. faecalis* strains and not the producing organism (source of target cells [lavender box], source of efagin [OG1RF, top row; isogenic OG1RF(*Δefg*) bottom row). **d,** Efagin dilution does not result in discrete plaque formation but breakthrough growth instead.

Efagin is selectively antimicrobial

Previous work[7] systematically explored seven putative prophage-related sequences moored within the prototype *E. faecalis* VRE V583 chromosome, including then-annotated partial phage-related element described here as efagin. All putative prophage-related sequences (alone or with added helper phage),

except for efagin, produced viable particles. Separately, as a byproduct of work assessing vesicle formation by *E. faecalis*, others[27] observed spurious copurifying particles which were attributed to genes of the efagin cluster, but the significance of those particles was not explored further.

Because efagin reading frames are well maintained and particles appeared to be expressed from them,[27] we undertook a search for activity. We reproduced the observations of Afonina et al.[27] by precipitating efagin exclusively from sterile culture filtrates of wild-type OG1RF and not from an isogenic strain generated here (OG1RF*Δefg*) in which the efagin gene cluster had been deleted, revealing phage tail-like particles.

To detect activity, paired sterile filtrates of OG1RF or OG1RF*Δefg* were assayed for potential antagonistic activity using a known diverse panel of *E. faecalis* lineages.[28] Efagin-specific inhibition was observed for some *E. faecalis* but not others (Fig. 1c). Notably, efagin expressed by OG1RF did not kill the producer itself, but was active against select other *E. faecalis* strains. Furthermore, when serially diluted, efagin inhibitory activity was lost evenly (rather than forming fewer well-resolved individual plaques, as is typical of phages capable of self-replication and reinfection), with breakthrough growth at lower concentrations as seen with some antibiotics (Fig. 1d). Further, inhibition appeared confined to the spot of application on the lawn with little diffusion.

Efagin structure

By transmission electron micrography (TEM), efagin particles measure from 113-234 nm, with a mean of 163 ± 11.8 nm (Fig. 2).

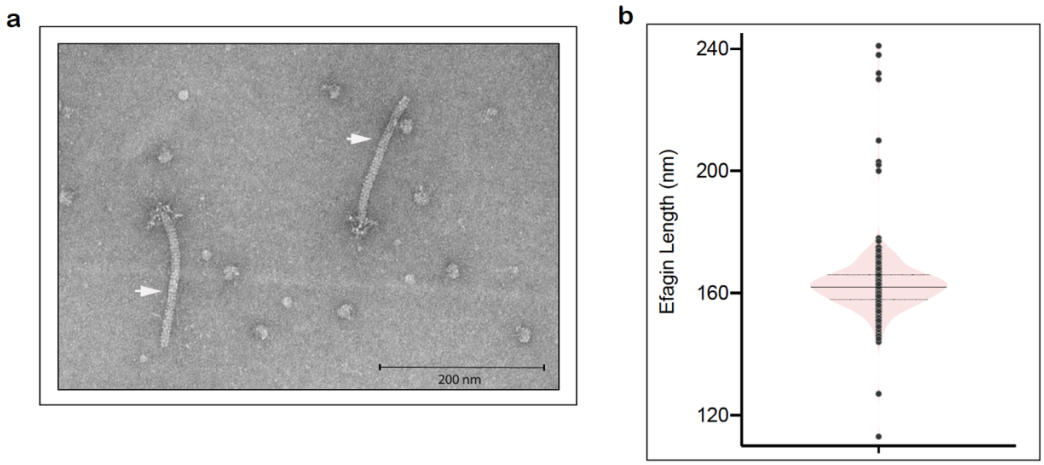

127

128 **Fig. 2. Efagin appears as a phage tail-like particle. a,** TEM image of OG1RF efagin particles (white
129 arrows) with phage tail-like structures including apparent baseplate. **b,** Size distribution of 300 efagin
130 particles.

131

132 ***ef1291* Sequence variation is non-random**

133 The observation of a concentrated patch of variability near the 3' end of one gene (*ef1291*) suggested
134 either a unique opportunity for sequence drift or selection for variation in the function encoded (Fig. 1b).
135 We therefore examined it closely and found that all variants fell into one of five patterns, termed efagin
136 types A-E (Fig. 3 and Table S14), supporting the latter prospect. Compared to (arbitrarily chosen) type A,
137 variations in types B, C, and D clustered around specific amino acid positions. In contrast, the C-terminus
138 of type E was unrelated (19.1% amino acid identity with type A) and appears to have arisen through
139 allelic substitution – based on sequence similarity, possibly with a phage of the *Caudoviricetes* group
140 (Table S15). We interpreted natural allelic replacement of this C-terminal domain to indicate that it likely
141 encodes an independently functional domain. Additionally, a subvariant (which we named type X) was
142 observed to occur within representatives of types B (2 subvariants), type C (49 subvariants), and type D
143 (2 subvariants). Each of these subvariants possesses small sequence perturbations resulting in a premature
144 stop codon that truncates EF1291 near the middle.

Efagin Types A-E

Type A (*E. faecalis* T9)
VTMPTVNGVP LESSRMAIYE ASGVGEVEAK YQAAFNKDNM KFVLIRVGNR VDAFVRCNLS DPTKLNNHMP KVFNIPTGYK MSSKISASVW NIPLSVAPYV FPYPNCNALY EIGNQGIIFA SSRAGNVYLQ GSWYTDDPFPTK*

Type B (*E. faecalis* T6)
VTMPTVNGLP LESSRMAIYE ASGVGEVEAK YQAAFNKVNM KFVLIRVGNR VDAFVRCNLS DPTKLNTHMP KIFNIPTGYK MSSKISASVW NIPLSVAPAA FPYPNCNALY EIGNQGIIFA SSRAGNVYLQ GSWYTDDPFPTK*

Type C (*E. faecalis* OG1RF)
VTMPTVNGVP FESSKMAIYE ASGVGEVGAK YQAAFNKDNM KFVLIRVGNR VDAFVRCNLS DPTKLNNNLV KVFTVPTGYT LSTKITKGIW NLALTAMQYT FPQPNCAGLY EMGNQGILFG ANRAGNIYLQ GSWYTDDPFPTK*

Type D (*E. faecalis* Com 1)
VTMPTVNGVP LESSKMAIYE ASGVGEVEAK YQAAFNKVNM KFVLIRVGNR VDAFVRCNLS DPTKLNSQVI KVFNVPTGYS INSVLKRNIW NIPLTAVQYN FPQPICTALY EIDNKGIIFC SNRAGNIYLQ GSWYTDDPFPTK*

Type E (*E. faecalis* T19)
SEAPLFKNLP LVSLGKFNLV GINGTEGSFT KVIGNMNNKE VGFGSDFSYI DERAKLANLN KNNNRLVIEE DGMYILIVHF WVQPITTVNG YWYFNFAING VRAGGPTDRF WGLGGTSWKN RQDGLGMVIR NFKKGDQLSA LIETNYTGEV NSTGIKSATLIKIG*

Fig. 3. EF1291 C-terminal sequence variation patterns. Variations in encoded amino acids 448 to 619 fall into distinct classes defining efagin types A-E (differences from type A highlighted in red). Type E appears to have arisen from recombination.

Structural similarity between EF1291 and a listeriophage carbohydrate-recognition domain

With limited inferred amino acid sequence identity to proteins of known function, we used Phyre2[29] to detect possible conserved structural motifs (Table S16). Phyre2[29] modeled 152 inferred C-terminal amino acids of efagin to the structure of the receptor-binding domain of Listeria phage PSA protein gp15 with 96.7% confidence. That domain of gp15 binds specific carbohydrate decorations on the variable *L. monocytogenes* wall teichoic acid (WTA).[30] We therefore used AlphaFold[31] to make a comparative efagin EF1291 model to map EF1291 sequence variations observed on its hypothetical structure (Extended Data Fig. 4). As listeriophage gp15 was solved in trimeric form,[30] a quaternary structure common to other phage target binding proteins,[32–34] EF1291 was modeled as a trimer as well. Variations defining efagin sequence types mapped to the positions of amino acids of gp15 including those known to contact specific carbohydrates of *Listeria* target cell WTAs[30] (Fig. 4).

The rhamnose-rich cell wall polysaccharide (Rha-CWPS) referred to as enterococcal polysaccharide antigen (Epa)[35,36], is the *E. faecalis* analog of the WTA targeted by listeriophage PSA protein gp15[30] and is also known to vary between strains.[37,38] Because the producing cell is not killed by its own efagin, we hypothesized that cells expressing various efagin types would possess different Epa cell wall carbohydrate structures to avoid self-targeting. We therefore tested covariation between the single

166 nucleotide polymorphisms (SNPs) encoding the EF1291 efagin type variations, and the presence/absence
167 of specific Rha-CWPS/*epa* operon genes indicative of alternate Epa structures, across the *E. faecalis*
168 species diversity. Significant correlations were found between select *ef1291* SNP positions and the
169 presence/absence of four genes in the *epa* cluster[36,38]: *ef2166* (-0.729, p=1.13e-91), *ef2167* (-0.729,
170 p=1.13e-91), *ef2168* (-0.723, p=1.46e-89); and *ef2169* (-0.698, p=6.05e-81) (Extended Data Fig. 5 and
171 Supplementary Fig. 2).

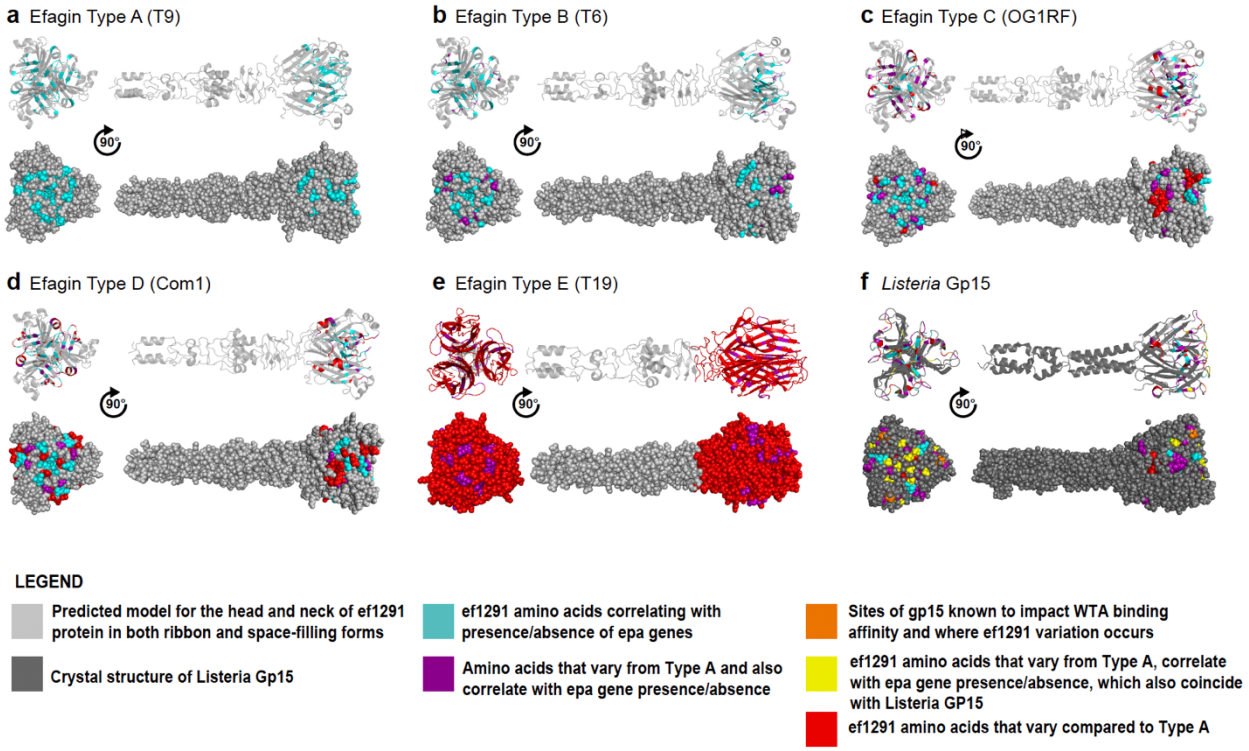

172

173 **Fig. 4. Structural similarities between EF1291 and listeriophage gp15 includes known carbohydrate-**
174 **recognition domain**. **a-e,** Base (left) and side (right) views of the predicted trimeric models of EF1291 in
175 efagin types A-E using Alphafold 3.[31] Amino acids that differ from efagin type A EF1291 are indicated in
176 red. Amino acids that correlate with the presence/absence of *epa* genes (correlation coefficient < -0.6) are
177 colored cyan. Amino acids that vary in both variation and correlation analysis are colored purple. **f,** Crystal
178 structure of listeriophage PSA gp15[30]. Amino acids known to impact WTA binding in gp15 are colored
179 yellow.[30] Orange amino acids are those known to impact WTA binding in gp15[30] and also vary in EF1291.
180

To experimentally verify Epa as the efagin target, we selected and sequenced efagin-resistant mutants of susceptible strains. Partially purified and concentrated type C efagin from OG1RF was spread onto lawns of susceptible *E. faecalis* strains FA2-2[39] and X98.[40] These targets were chosen because both are susceptible to type C efagin, but enigmatically were previously shown to be of different *epa* genotypes.[37] Four FA2-2 mutants (FA2-2R1-R4) and two X98 mutants (X98R1 and -R2) were chosen for genome sequence comparison to parental controls. All type C efagin resistant mutants of both lineages possessed mutations in *epa* operon genes (Table S17 and Extended Data Fig. 6), providing direct experimental evidence that despite differences in *epa* genotype, wild type Epa is necessary for efagin activity.

Building on a prior analysis,[37] we re-examined the diversity of *epa* operons in 1,972 high quality *E. faecalis* genomes. The *E. faecalis epa* cluster consists of 18 conserved core genes (*epa*A–*epa*R) followed by variable genes downstream (with *ef2164* to *ef2198* constituting the variable *epa* genes of prototype VRE *E. faecalis* strain V583)[36,37] (Table S18). Therefore, the diversity of *epa* operons was clustered based on the extent of shared homologs in the variable gene set, which identified 20 *E. faecalis epa* genotypes (Fig. 5 and Table S14). All four genes whose presence or absence covaried with type-defining efagin variations (*ef2166–ef2169*) are widely shared but not universal in the variable gene set (Fig. 5).

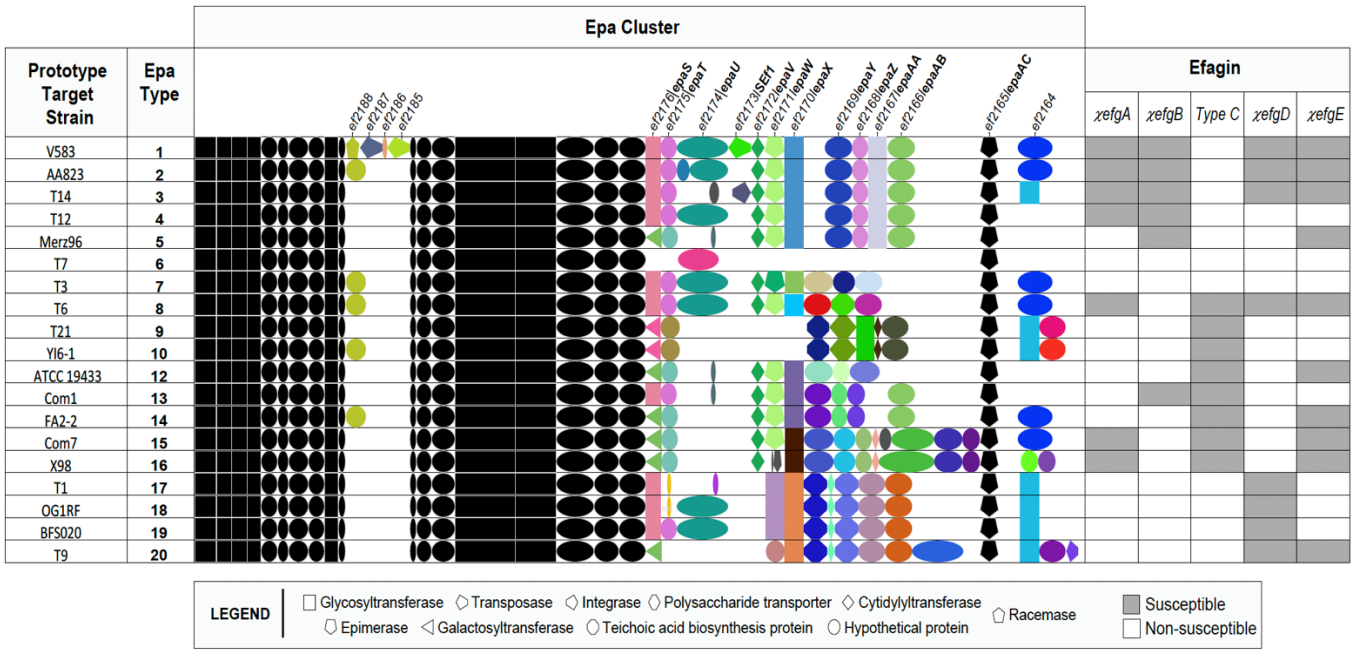

197 **Fig. 5. Epa genotypes and their susceptibility to targeting by efagin types.** Representative operons of
198 19 of 20 identified *epa* genotypes occurring in strains available to us are symbolically represented (black
199 [core] and colored [variable] shapes correspond to predicted function). Susceptibility to inhibition of each
200 *epa* genotype strain to efagin types A-E is indicated (grey boxes), as measured using chimeras constructed
201 on the OG1RF type C background to control for other potential antimicrobial activities potentially
202 expressed by natural producers. Chimeras are labeled using the Greek letter "χ"(*chi*), followed by efagin
203 (*efg*) type.
204

205 **The EF1291 C-terminal domain determines target cell specificity**

206 To prove that the C-terminal domain of EF1291 determines target cell specificity, chimeras possessing C-
207 terminal domain swaps from EF1291 sequence variation type A, B, D, and E donors, were constructed on
208 the efagin type C background of OG1RF by allelic replacement.[41] This allowed assessment of efagin
209 activity and targeting free of other potential antagonistic activities or phages common in wild-type
210 natural producers. Generation of an efagin type D EF1291 C-terminal chimera proved initially difficult.
211 We reasoned that efagin type D may target OG1RF, making such a construct suicidal. Direct assessment
212 of the supernatant of the type D (C-terminus donor strain Com1) supported this prospect (although other
213 potentially Com1-expressed inhibitory activities were not controlled for). Nevertheless, using partially
214 purified Com1 efagin to select for resistant OG1RF mutants, two independently derived colonies were
215 selected for genome sequence analysis, OG1RF-R1 and OG1RF-R2. Consistent with expectation, each
216 possessed a different mutation in the OG1RF *epa* operon variable region (Extended Data Fig. 6 and Table
217 S17). Strain OG1RF-R2 was arbitrarily selected as the host for construction and expression of the type D
218 chimera, which was obtained without further difficulty. Once obtained, the type D chimera was verified
219 as targeting OG1RF, but not OG1RF-R1 and -R2 mutants. Each chimeric construction (termed χ*efg*A, B,
220 D, and E, respectively) was obtained on the OG1RF type C efagin background and verified by
221 sequencing. Construction of EF1291 chimeras did not detectably affect efagin assembly or structure
222 (Supplementary Fig. 3)

223 Each efagin chimera was systematically examined for altered target cell specificity using representatives
224 of 19 of the 20 *epa* genotypes identified (Fig. 5), as we were unable to obtain an *epa* genotype 11 strain
225 for testing (Supplementary Fig. 4). Chimeric efagins χ*efg*A, χ*efg*B, χ*efg*D, and χ*efg*E exhibit distinct
226 target cell specificities showing both functionality and altered specificity. Efagins show overlapping
227 activity patterns, but each type displays unique activities. This indicates that each efagin targets a unique
228 aspect of the variable and complex Rha-CWPS/Epa structure, [42,43] as well as more broadly shared
229 elements. As an additional proof of targeting, χ*efg*A was used to select for resistant mutants of its
230 prototype strain target, V583. Again, two mutants were obtained and sequenced, V583-R1 and -R2, and
231 again both also possessed mutations in variable region genes of its *epa* operon (Extended Data Fig. 6 and
232 Table S17). All strains targeted by chimeras were confirmed to also be targeted by filtrates of the donors
233 from which the *ef1291* sequence originated.

234 **Efagin/Epa compatibility as a driver of horizontal gene exchange**

235 Gene clusters encoding efagin (in *E. faecalis* V583, *ef1276 – ef1293*) and Epa (*ef2198 – ef2164*) are not
236 linked and separated by approximately 1/3rd of the genome. We never detected a population collapse
237 associated with efagin production by an *E. faecalis* strain, nor do chimeric efagins kill the strains from
238 which the corresponding C-terminal encoding sequence derived (Fig. 5), indicating that its ecological role
239 is not likely fratricide.[44] We therefore examined patterns of co-occurrence of efagin and corresponding
240 *epa* genotypes in 493 *E. faecalis* genomes representing all major phylogenetic branches across the species
241 (Supplementary Fig. 5). As predicted, the results reveal a non-random pattern with certain pairings
242 occurring at high frequency (*e.g.*, efagin type B and *epa* type 8; or efagin type C and *epa* type 1), while
243 others appear less common but still permissible. Both efagin types and *epa* genotypes are scattered across
244 the whole genome-based phylogeny (Supplementary Fig. 6), these co-occurrences support a functional
245 linkage and possible co-evolution between efagin and *epa*, likely shaped by selective pressures related to
246 self-immunity.

247 The association between efagin type and a non-targeted *Epa* genotype in the producing cell was found to
248 be highly significant, providing further support for a model where efagins target Epa types heterologous
249 to that of the producer (Fisher's exact test $p < 0.00001$) (Extended Data Fig. 7 and Table S19). However,
250 exceptions were observed, both implying unexpected susceptibility as well as resistance (Extended Data
251 Fig. 7). For example, strain SS7 (*epa* type 9) was found to be resistant to killing by efagin type C,
252 whereas other members of *epa* type 9 were found susceptible. Close examination of the SS7 chromosome
253 shows that it harbors an additional gene within the *epa* operon (Extended Data Fig. 7, orthogroup 151;
254 pink), potentially modifying its Epa structure. Other exceptions without obvious gene gains or losses
255 (*e.g.*, strain Fly2, *epa* operon type 1 but resistant to efagin type D) likely have more subtle changes such
256 as point mutations that affect expression of specific genes within their *epa* operons, as was found in
257 experimentally derived resistant mutants, but this remains to be shown.

258 **Efagins and phages select for cross-resistance**

259 Chatterjee and colleagues[45] observed that mutants of *E. faecalis* strain X98 gained immunity to infection
260 by some phages after acquiring mutations in *epa* genes. We obtained two mutants (51RS1 and 51RS2)
261 from that study to test for alteration in efagin susceptibility. Wild type X98 is targeted by efagin types A,
262 C, and E (Extended Data Fig. 6). Phage-resistant mutant 51RS1 (with lesion in the *epa* gene
263 EFOG_0058[45]) retains susceptibility only to types A and E, but not type C, whereas phage-resistant X98
264 mutant 51RS2 (with lesion in *epa* gene EFOG_0052)[45] is resistant to all efagin types (Extended Data Fig.
265 6). This shows that phage selection contributes to variation in efagin susceptibility and likely vice versa.

266 **Efagin target range extends beyond *E. faecalis* to other enterococcal species**

267 We previously identified structural similarities between the *epa* operons of *E. faecalis*, *E. faecium*[37] and in
268 the related operons of other *Enterococcus* species.[38] It therefore was of interest to determine whether
269 efagin activity extends beyond *E. faecalis*. A collection of 58 *E. faecium* genomes spanning the species[46]
270 was assessed for efagin susceptibility *E. faecium epa* operons also possess a conserved and then variable
271 genes and assessment of their diversity was updated using currently available data (Extended Data Figs. 8

272 and 9; Tables S20 and S21). Of those 58 diverse strains, 35 were found to be susceptible to at least one
273 efagin type (Extended Data Fig. 9). Interestingly, 39% of VRE *E. faecium* (7/18) are targeted by an
274 efagin, whereas 70% (28/40) of VSE *E. faecium* are susceptible. Importantly, only 6% (1/16) of the
275 highly successful and often VRE clonal complex 17 (CC17) lineage is targeted by an efagin. As both *E.*
276 *faecalis* and *E. faecium* species co-occur in the human gut,[47] this raises the prospect that evolving cellular
277 surfaces resistant to efagin inhibition may have contributed to the ecological success of the VRE *E.*
278 *faecium* CC17 lineage.

279 In addition to *E. faecium*, 40 other *Enterococcus* species spanning all four phylogenetic clades[1,5] were
280 evaluated for efagin susceptibility (Extended Data Fig. 10 and Table S22). Efagins were found to be
281 effective against many species within clades I, II, and III, predominantly species possessing *epa* genes
282 closely related to those of *E. faecalis*. In contrast, many clade IV species lack close homologs to genes for
283 synthesis of the core rhamnopolysaccharide stem of Epa,[38,42] and their Rha-CWPS/*epa* operon
284 counterparts have received little study. Interestingly, *E. testudinis* was found to be susceptible to efagin
285 despite lacking detectable sequence identity to core or variable *epa* genes of *E. faecalis* V583, suggesting
286 the presence of a distinct cell wall polysaccharide structure that nevertheless possesses terminal
287 decorations, or perhaps other cell wall structures, that serve as a binding target for efagin type C.

288

289 **DISCUSSION**

290 Here we identify efagins as a new class of independently evolved, selective microbial inhibitors core to the
291 biology of *E. faecalis*. A phage tail fiber-like protein, EF1291, targets efagins to variation in enterococcal
292 cell wall Rha-CWPS Epa which is common to most but not all enterococcal species. Whether functional
293 targets occur on microbes with non-rhamnose-based carbohydrate structures on their surface is currently
294 unknown, but appears possible based on the observed inhibition of *E. testudinis*. With activity against *E.*
295 *faecium* strains, including some VRE clinical isolates, and the demonstrated ability to engineer specificity
296 through discrete domain swaps, such agents and potentially engineered derivatives hold promise for

297 selectively controlling infection as well as the gut ecology of hospitalized patients limiting transmission
298 and spread.

299 The discovery of efagins provides a new perspective on *E. faecalis* ecology and evolution as well. Their
300 conservation in all *E. faecalis* and their uniqueness to that species imply that they were either gained at the
301 time of species radiation over 300 million years ago[1] and transmitted vertically, or later acquired and spread
302 throughout a population sweep. Their invariant occurrence in widely ranging ecologies, and absence outside
303 of that species, argue strongly for the former. With activity against competing strains of many enterococcal
304 species, efagins appear well suited to facilitate *E. faecalis* entry into diverse gut consortia. That is, as
305 animals along with their microbes are consumed up the food chain, *E. faecalis* in prey may deploy efagins
306 in the gut of a predator to displace competitors. As facile gene exchangers[48] the escalation of *E. faecalis* up
307 the food chain from a vast range of ecosystems positions them ideally to be important conduits of adaptive
308 traits from various ecosystems, including naturally occurring antibiotic resistance genes.

309 Cross selection and coevolution of efagins, phages and their Epa targets has likely contributed to *E. faecalis*
310 genetic diversity. Here, we observed that the evolutionary dynamics of the efagin and *epa* differ from much
311 of the rest of the core genome, raising the prospect that efagin-mediated selection may represent a new
312 important driver of gene exchange. Efagin susceptibility patterns across varying *epa* operon genotypes
313 likely mirror phage susceptibility patterns, substantially informing the development of phages for
314 therapeutic purposes as well.

315 The discovery of efagins provides yet another independently derived example of what is often viewed as
316 the co-option and redeployment of a phage structure for the selective advantage of a bacterium.[49] However,
317 as for other phage component-like bacterial factors, the paucity of intermediates makes it difficult to
318 substantiate a precise evolutionary pathway, making it entirely possible if not likely that the independent
319 utility of tail-like (or alternatively capsid-like) functional units has simply been co-opted in parallel by
320 microbes and viruses for various cellular and viral uses. [50]

321 As for tailocins, [15,18,21,24,49,51] we show that efagins are capable of inhibiting the growth of targeted strains
322 under the conditions tested here. However, much remains to be learned about the actual ecological role of
323 efagins in nature. The precise mechanism of action for efagins, as for other non-contractile F-type tailocins,
324 is unclear[18,21,22]. If competitor killing or inhibition is the objective, the nature of the selection that favors a
325 160 nm tail polymer is also unclear, when a) shorter variations spontaneously occur, and b) killing involves
326 activities mainly of the baseplate.[22]

327 Much remains to be learned about the contributions of efagins to the biology of *E. faecalis*, and their
328 contribution to its exceptional success – both as a commensal of a wide range of terrestrial animal guts and
329 as a persistent, multidrug resistant hospital pathogen. Irrespective of their role in nature, they clearly possess
330 the ability to be engineered to target cells expressing a cognate cell wall rhamnopolysaccharide (and
331 possibly related structures), which may be of considerable value in managing and limiting the spread of
332 multidrug resistant enterococci in medical and agricultural environments. In an era when few effective
333 treatment options remain for those with multidrug resistant enterococcal infections, the identification of a
334 new agent that targets these recalcitrant organisms represents an important advance.

335

336 **METHODS**

337 **Collection of bacterial strains**

338 The bacterial collection used in the experimental work is described in Tables S23, S24, S25, and S26.
339 *Enterococcus* species were propagated in Brain Heart Infusion (BHI) broth or on 1.5% BHI agar at 34 °C
340 or 37 °C, depending on temperature preferences for each species[5], while *Vagococcus giribetii* was
341 incubated at 34 °C. *Escherichia coli* was maintained on 2x Yeast Tryptone medium (2xYT) at 37 °C.

342 **Induction and recovery of efagin particles**

343 To obtain efagin particles, bacterial cultures were grown overnight in BHI broth and incubated at 37 °C
344 for 18 h. For strains not expressing efagin constitutively, overnight cultures were diluted 1:100 in BHI

345 broth and incubated for 4 h, followed by induction with mitomycin C (final concentration 2.5 µg/ml) and
346 incubation at 37 °C overnight. The cell debris was removed by centrifugation at 11,000 × *g* for 15
347 minutes at 4 °C. Then the supernatant was collected and filtered through a 0.2 um membrane (Pall Life
348 Sciences). Efagin particles collected in the supernatants were added along with 1 M NaCl (5.84 g/100 ml)
349 and 10% (w/vol) polyethylene glycol 8000 (PEG), and the mixture was incubated for 1h at 4 °C. The
350 PEG-precipitated material was then collected by centrifugation at 25,000 × *g,* 4 °C, for 1 h. The pellet
351 was resuspended in SM buffer (50mM Tris-Cl pH 7.5, 100 mM NaCl, 8mM $MgSO_4$•$7H_2O$,) and another
352 addition of 2.5 M NaCl and 20% (w/v) polyethylene glycol PEG-8000 was performed for 30 min at room
353 temperature. Efagin particles were collected by centrifugation at 17,000 × g, 4 °C, for 1 h, and the pellets
354 were resuspended in SM buffer.

355 **Efagin purification and concentration**

356 Efagin particles were purified and concentrated using centrifugal filter units: Macrosep 100 K MWCO
357 advance centrifugal devices (20 ml; Pall Life Sciences), and Amicon Ultra 100K; (0.5 ml; Millipore)
358 according to the manufacturer's instructions. Briefly, efagin suspensions in SM buffer were loaded into
359 Macrosep 100 K and centrifuged at 4,000 × g for 1.5 h. The collection tubes were then emptied, refilled
360 with 10 mL SM buffer, and subjected to a second centrifugation step. Retained particles were
361 resuspended in 2 mL SM buffer and transferred to Amicon Ultra 100 K filters. These were centrifuged at
362 5,000 × g for 30 min, and efagin was recovered by reverse spinning at 1,000 × g for 2 min. The resulting
363 concentrated preparations were used for activity assays of efagin and for subsequent analyses.

364 **Transmission Electron Microscopic (TEM)**

365 Purified efagin particles were diluted in SM buffer to a concentration of 10^7 efagin-forming units/ml.
366 Freshly ionized carbon coated grids were floated on a 10 ul drop of sample for 1 minute. Grids were
367 washed with 5 drops of 2% uranyl acetate (UA), and the excess of UA was drawn off with grade 50
368 Whatman filter paper. Grids were allowed to dry and imaged with a Hitachi 7800 at 100KV.

369 **Grids preparation and imaging conditions for single particle analysis**

370 Purified efagin particles in a volume of 3 µl were applied onto the glow discharged Quantifoil R 1.2/1.3,
371 300 Mesh, Au grid and plunge frozen using the Vitrobot Mark 4 (Thermo Fisher Scientific, Waltham,
372 MA, USA) in 100% humidity and 4°C. The grids were blotted for 3s and automatically plunged into
373 liquid ethane. Vitrified samples were transferred to storage boxes and stored in liquid nitrogen until use.
374 Grids were clipped in AutoGrid Rings and loaded into a 300 kV Titan Krios electron microscope (Thermo
375 Fisher Scientific, Waltham, MA, USA) with Gatan K3 Camera and BioQuantum Energy Filter set to a 20
376 eV slit width. Micrographs were collected with a nominal 81.000x magnification, with a corresponding
377 pixel size of 1.065Å, a total dose equal 60e-/Å, 50 frames and defocus range of -2.1 to -0.9 µm.

378 Micrographs were imported to the CryoSPARC v4.6 software,[52] followed by Patch Motion Correction
379 and Patch CTF Correction. Three hundred random efagin particles were manually measured, which
380 allowed us to prepare the length distribution plot using RStudio v2025.09.2 software.[53]

381 **Detection of phage activity and titration**

382 Efagin particles from OG1RF *E. faecalis* were tested on an indicator strain for plaque formation.[54]
383 Briefly, the indicator strain was cultured overnight and then diluted to equal the turbidity of a 0.5
384 McFarland standard (~1.5 x 10^8 colony forming units (CFU)/ml). One hundred microliters of the bacterial
385 suspension were mixed with 1 ul of diluted efagin particles (prepared 10 to 10^9-fold serial dilutions) and 5
386 ml of 0.5% BHI agar, which was then poured onto a 1% BHI agar plate. Once the overlay solidified, the
387 plates were air-dried and incubated overnight at 37 °C. Plaque formation was visually detected and
388 enumerated by plaque assay using JM110 *Escherichia coli* (indicator strain) and M13 bacteriophages as
389 the positive control.

390 **Efagin locus knockout in *E. faecalis* OG1RF**

391 An efagin knockout strain of *E. faecalis* OG1RF was generated through allelic replacement. Genomic
392 regions flanking the efagin locus (878 bp upstream and 860 bp downstream) were amplified by PCR
393 using primer pairs KO-F1_XbaI up-forward/KO-R1_Acc65I up-reverse and KO-F2_KpnI down-
394 forward/KO-R2_SbfI down-reverse (Table S27), then fused via overlap extension PCR to create a 1,738

395 bp deletion construct. This fragment was digested with *XbaI*/ *SbfI* and cloned into the temperature-
396 sensitive plasmid pLT06 pre-digested with the same enzymes. The recombinant plasmid was propagated
397 in *E. coli* EC1000 and verified by sequencing. Following PCR confirmation with primers OriF and
398 KS05seqR, the construct was introduced into *E. faecalis* OG1RF by electroporation. Allelic exchange
399 was carried out using temperature shift and p-chlorophenylalanine counterselection, as described
400 previously.[41] Candidate mutants were screened by PCR using internal primers (efagin-internal-F and
401 efagin-internal-R; **Table S27**), and successful deletion was confirmed by whole genome sequencing.

402 **Construction of efagin chimeras in *E. faecalis* OG1RF**

403 Efagin chimeras of *E. faecalis* OG1RF were generated by allelic exchange. A 1,324 bp DNA fragment
404 spanning the region between the C-terminal end of *ef*1291 and the start of the EF1292 efagin gene was
405 amplified by PCR using primer pair 817_F_BamHI up-forward/2150_R_PstI up-reverse (Table S27). The
406 resulting product was digested with BamHI and PstI and ligated into the temperature-sensitive plasmid
407 pLT06, pre-digested with the same enzymes. Recombinant plasmids were propagated in *E. coli* EC1000
408 in medium supplemented with chloramphenicol (15 µg/mL), verified by PCR using primers OriF and
409 KS05seqR, and confirmed by Sanger sequencing. Plasmids were subsequently extracted and introduced
410 into *E. faecalis* OG1RF by electroporation. Allelic exchange was carried out using temperature shift and
411 p-chlorophenylalanine counterselection, as previously described.[41] Candidate mutants were screened by
412 PCR using internal primers for efagin types A–E (internal-F and internal-R; Table S27) and further
413 evaluated by activity assays. Successful recombinants were validated by sequencing.

414 **Host range determination**

415 Efagin killing assays were conducted using spot tests and the double agar layer method. [55] The indicator
416 strains were cultured overnight and then diluted to equal the turbidity of a 0.5 McFarland standard (~1.5 x
417 10^8 CFU/ml). One hundred microliters of the bacterial suspension were applied to a 0.5% Brain Heart
418 Infusion (BHI) agar overlay, which was then poured onto a 1% BHI agar plate. Once the overlay
419 solidified, the plates were air-dried and incubated in the refrigerator for 1 hour. Following this, 4 µl of

420 efagin preparations were carefully spotted onto the plates and allowed to dry/adsorb and incubated at 4°C
421 for 2h. After that, the plates were incubated at 37 °C overnight, and zones of clearing indicated positive
422 bactericidal activity.

423 **Isolation of efagin-resistant *E. faecalis* strains**

424 The efagin-resistant phenotypes were selected using spot tests and the double agar layer method as
425 described previously. Plates were let dry, and 4-20 µl of efagin particles were spotted and allowed to
426 dry/adsorb for 4 h. After, plates were incubated at 37 °C overnight. The presumptive efagin-resistant
427 colonies appeared in the zones of clearing. The efagin-resistant phenotypes were confirmed by spot
428 assays and whole genome sequencing (WGS).

429 **Genomic DNA preparation, high-Throughput sequencing, assembly, and annotation**

430 *Enterococcus* strains were cultured in BHI broth at 37 °C for 18 h. Genomic DNA was extracted using the
431 DNeasy Blood & Tissue Kit (QIAGEN, San Luis, MO, USA) with minor modifications to the
432 manufacturer's protocol. Specifically, 50 µL of lysozyme (50 mg/mL) and 10 µL of mutanolysin (2,500
433 U/mL; Sigma-Aldrich, Germantown, MD, USA) were added and incubated for 30 min at 37 °C prior to
434 treatment with 20 µL proteinase K (20 mg/mL). DNA concentrations were determined using the Qubit
435 dsDNA High-Sensitivity Assay Kit (Thermo Fisher Scientific, MA, USA). Sequencing libraries were
436 prepared with the Nextera XT DNA kit and Illumina index primers. Paired-end reads (2 × 250 bp) were
437 generated on an Illumina MiSeq platform with the MiSeq Reagent Kit v2. Reads were trimmed to remove
438 adapters, quality-filtered, and screened for PhiX contamination before de novo assembly in CLC
439 Genomics Workbench v8.0.3. Ten additional strains (efagin resistant-mutants and chimeras) were
440 sequenced externally by CD Genomics (https://www.cd-genomics.com) and processed using the same
441 pipeline.

442 All Illumina sequencing reads and assembled genomes have been deposited in GenBank under
443 BioProjects PRJNA313452[56] and PRJNA663900,[57] and PRJNA1371623[58]. Strains and corresponding
444 accession numbers are provided in Table S1.

445 **WGS variant calling analysis**

446 Whole-genome sequencing was performed on both efagin-resistant mutants and their corresponding
447 parental strains to identify single nucleotide polymorphisms (SNPs) and insertions/deletions (indels).
448 Sequencing reads were aligned to the finished reference genome using the BWA-MEM algorithm
449 (v0.7.4).[59] Variant calling was then carried out using Pilon **(**v1.23).[60] Variants with a mapping quality
450 score below 10 were excluded from the final dataset to ensure accuracy.

451 **Searching for efagin sequence in Enterococcaceae and other prokaryotic bacteria**

452 We downloaded all 16,907 Enterococcaceae assemblies (Taxid 18,015) from NCBI
453 (https://www.ncbi.nlm.nih.gov), in May 2021, to analyze together with additional Enterococcaceae
454 genomes from the Broad Institute's collection (n= 1108). Quality controls were performed to remove
455 contaminated or incomplete genomes, using Phylosift[61] and CheckM.[62] FastANI[63] was used to identify
456 species in our dataset by comparing to reference genomes, including *E. faecalis* V583, with the presence
457 of >95% average nucleotide identity to a known reference genome confirming the species designation.
458 Our final dataset contained 15,854 confirmed Enterococcaceae assemblies for analysis, including 3,068 *E.*
459 *faecalis*.

460 BLAST (https://www.ncbi.nlm.nih.gov) was used to search our enterococcal assembly database for hits
461 matching the efagin sequence from *E. faecalis* reference strain V583. We calculated the total coverage of
462 efagin for hits within each target sequence, accounting for overlapping hits. Efagin was defined as present
463 in a strain if there were Blast hits with at least 90% coverage of efagin (E-value <10), including at least
464 one hit of length > 2000 bp. Another, more comprehensive BLAST search was performed against all draft
465 prokaryotic genomes available on NCBI (https://www.ncbi.nlm.nih.gov). All sequencing submissions
466 matching the query "wgs_master[prop] AND (bacteria[orgn] OR archaea[orgn]) NOT refseq[filter]" on
467 the NCBI Nucleotide website were included in this dataset (https://www.ncbi.nlm.nih.gov), or
468 approximately 1.2 million sequencing submissions in Oct 2022.

469 **Selection of representative *E. faecalis, L. monocytogenes, P. aeruginosa and C. difficile* genomes to**
470 **cover the breadth of diversity within the species**

471 In order to remove biases within our dataset due to over-representation of commonly sequenced clinical
472 subtypes, and to ensure computational tractability, we selected representative genomes for each species,
473 chosen to represent the diversity present across the species. Briefly, all genomes were clustered using the
474 StrainGR (v1.3) software package[64], using its utility for creating representative reference genome
475 databases. We clustered genomes with a jaccard distance of 0.9, and a representative was chosen for each
476 cluster.

477 For *E. faecalis*, we started with our full set of 3,068 genomes. After clustering, we chose the
478 representatives with the smallest number of contigs, that also contained a full efagin on a single contig,
479 resulting in a set of 441 *E. faecalis* genomes. Additionally, we added lab-tested strains important to this
480 study, with a final total of 493 genomes representing the diversity of *E. faecalis*.

481 For analyses of *Listeria monocytogenes*, *Pseudomonas aeruginosa*, and *Clostridium difficile*, we started
482 with 414, 883 and 189 genomes from the complete refseq database, respectively. After clustering, the
483 resulting datasets contained 74, 343, and 32 genomes, respectively, highlighting different levels of
484 diversity for each species in the database.

485 **Searching for partial phages**

486 To detect partial phages from additional enterococcal species and closely related *Melissococcus plutonius*,
487 *Tetragenococcus halophilus*, and *Vagococcus fluvialis*, we used all isolates for each species from the
488 refined dataset of 15,854 Enterococcaceae assemblies described above. These were then used as input into
489 the provirus identification tool within the geNomad software package. [10] This tool identifies and extracts
490 proviruses from assembled genomes by detecting regions enriched in viral hallmark genes using
491 genomad's neural network classification model. We filtered for proviruses present in the majority of
492 isolates in each species and explored whether they lack typical prophage proteins using geNomad[10].
493 Incomplete annotations were confirmed with Phastest.[11]

494 **Identification of the closest known ancestor of efagin and protein identity**

495 All V583 efagin gene sequences were analyzed using the phage prediction tool PHASTER[65] and
496 Phastest[11] to identify the closest known phage ancestor. The resulting phage protein sequences were then
497 compared with efagin proteins using BLAST alignments (default E-value thresholds) to determine
498 protein-level identity.

499 **Monocin similarity analysis**

500 Using nucleotide sequences from all V583 efagin genes, we searched against the monocin gene sequences
501 and obtained no hits (default E-value thresholds). Using sequences from all V583 efagin proteins, we
502 searched against the monocin protein sequences from ATCC 35152 strain using a BLAST e-value
503 threshold of 1e-5.

504 **Functional annotation of efagin and genes in its genomic neighborhood**

505 Gene function information for efagin (*ef1276* to *ef1293*) and its surrounding region (20 genes upstream
506 and downstream) was obtained by combining information from Prokka,[66] Pfam,[67] Kegg,[68] Phyre 2.2,[29]
507 BioCyc,[69] Alphafold 3,[31] and PaperBlast.[70] The annotated genes immediately upstream and downstream
508 of *efagin* via this pipeline are not present in the *E. faecalis* V583 genome annotation in GenBank
509 (https://www.ncbi.nlm.nih.gov), but were found in our Prokka[66] annotations. For reference in our
510 analysis, we assigned them arbitrary *ef* IDs: *ef3441* (upstream) and *ef3442* (downstream).

511 **Orthogroup clustering and characterization of *epa***

512 To obtain efagin particles, bacterial cultures were grown. Among all isolates containing a complete efagin
513 sequence, 1,972 also had a complete epa operon on one contig. Since *epa* consists of a conserved region
514 followed by a variable region (containing 7 to 27 genes), a conserved gene downstream of *epa*, *ef2162*,
515 was used to define the downstream boundary of the operon. The genes between *epa*A and *ef2162*, not
516 including *ef2162*, were considered part of the *epa* operon and were included in our orthogroup clustering
517 analysis. SynerClust[71] was run on these genomes, classifying all *epa* genes into 137 orthogroups. To

518 further correct for possible overclustering artifacts, we split orthogroups with within-cluster average
519 nucleotide identity <90%.

520 To explore the presence of *epa* in *E. faecium*, we downloaded 58 diverse *E. faecium* genomes from a
521 previously published study[46] and repeated the same orthogroup clustering process described above. In
522 total, 95 epa orthogroups were present in *E. faecium*.

523 In order to understand epa diversity across the *Enterococcus* genus, we used previously published
524 results[38] that used BLAST to identify which epa genes are present in other enterococcal species,
525 calculating the percent identity between genes from different enterococci and the *E. faecalis* V583 epa
526 genes. For new isolates not included in that study,[38] we also used the same method to detect epa genes,
527 using the same E-value threshold of 1E-10 for inclusion as a positive hit.

528 **Analysis of correlation between efagin SNPs and *epa* genes**

529 For each gene in the variable region of the epa, we created a vector with a binary value corresponding to
530 the presence or absence of this gene within each *E. faecalis* representative genome selected as described
531 above. Correspondingly, for each 150bp region within efagin, we created a vector containing the number
532 of SNPs in that region for each representative genome within our database. A position in a genome was
533 considered a SNP if it differed from the nucleotide at that position in V583 or if it was an inserted or
534 deleted relative to V583. Pearson correlations were calculated between the vectors for each epa gene and
535 each efagin region.

536 **Protein structural modeling**

537 Alphafold 3[31] was used to model the full-length protein structures of all five efagin *ef*1291 types via
538 alphafoldserver.com. As gp15[30] is known to form a homotrimeric structure, we included three copies of
539 *ef*1291 as input. We generated visualizations using Pymol.[72]

540 **Defining Epa and efagin types**

541 We defined epa types using hierarchical clustering, based on the presence or absence of *epa* genes in our
542 orthogroup clustering based on 1,972 *E. faecalis* genomes. This was performed using the
543 AgglomerativeClustering package from scikit-learn.[73] We chose an optimal threshold by comparing the
544 clusters with patterns of efagin killing activity, achieving optimal agreement with the distance_threshold
545 parameter value of 9. For the 58 *E. faecium* genomes, we applied the same approach, using a
546 distance_threshold parameter value of 6.

547 Efagin types were defined for the complete dataset using hierarchical clustering of an alignment of amino
548 acid residues representing the variable region of *ef*1291 (V583 efagin coordinates 12,539-12,967). We
549 used the AgglomerativeClustering package,[73] and an optimal threshold was chosen by comparing the
550 clusters with patterns of efagin killing activity, achieving optimal agreement with a distance_threshold
551 value of 24.

552 **Construction of phylogenies**

553 The whole-genome phylogeny of *E. faecali*s representatives was generated with Parsnp v1.1.2 [2]/23/26
554 4:23:00 PM using default parameters and V583 as the reference genome. To construct the single-copy
555 core phylogenetic tree of Enterobacteriaceae, individual representative genomes for each species were
556 used as input to Orthofinder[74] to find all genes present in >=95% of isolates. These were aligned with
557 MAFFT[75] and then phylogenetically reconstructed using IQTree[76] in modelfinder mode with 1000
558 ultrafast bootstraps.

559 **Data availability**

560 All Illumina sequencing reads and assembled genomes have been deposited in GenBank under accession
561 numbers BioProjects PRJNA313452[56], PRJNA663900[57], and PRJNA1371623[58]. Strains and
562 corresponding accession numbers are provided in Tables S1. Any additional information required to
563 reanalyze the data reported in this paper is available from the lead contact (Michael S. Gilmore;
564 michael_gilmore@meei.harvard.edu) upon request.

565

566 **REFERENCES**

567 1. Lebreton, F. *et al.* Tracing the Enterococci from Paleozoic Origins to the Hospital. *Cell* **169**, 849-
568 861.e13 (2017).
569 2. *Centers for Disease Control and Prevention (CDC). Antibiotic Resistance Threats in the United*
570 *States.* https://www.cdc.gov/antimicrobial-resistance/data-research/threats/index.html.
571 3. Ikuta, K. S. *et al.* Global mortality associated with 33 bacterial pathogens in 2019: a systematic
572 analysis for the Global Burden of Disease Study 2019. *The Lancet* **400**, 2221–2248 (2022).
573 4. *European Centre for Disease Prevention and Control - ECDC (2024). Antimicrobial Resistance in*
574 *the EU/EEA (EARS-Net)—Annual Epidemiological Report 2023. November 18, 2024.*
575 https://www.ecdc.europa.eu/en/publications-data/antimicrobial-resistance-eueea-ears-net-annual-
576 epidemiological-report-2023.
577 5. Schwartzman, J. A. *et al.* Global diversity of enterococci and description of 18 previously unknown
578 species. *Proc. Natl. Acad. Sci.* **121**, e2310852121 (2024).
579 6. Paulsen, I. T. Role of Mobile DNA in the Evolution of Vancomycin-Resistant Enterococcus faecalis.
580 *Science* **299**, 2071–2074 (2003).
581 7. Matos, R. C. *et al. Enterococcus faecalis* Prophage Dynamics and Contributions to Pathogenic Traits.
582 *PLoS Genet.* **9**, e1003539 (2013).
583 8. Scholl, D. Phage Tail–Like Bacteriocins. *Annu. Rev. Virol.* **4**, 453–467 (2017).
584 9. Backman, T., Burbano, H. A. & Karasov, T. L. Tradeoffs and constraints on the evolution of
585 tailocins. *Trends Microbiol.* **32**, 1084–1095 (2024).
586 10. Camargo, A. P. *et al.* Identification of mobile genetic elements with geNomad. *Nat. Biotechnol.* **42**,
587 1303–1312 (2024).
588 11. Wishart, D. S. *et al.* PHASTEST: faster than PHASTER, better than PHAST. *Nucleic Acids Res.* **51**,
589 W443–W450 (2023).

590 12. Bobay, L.-M., Touchon, M. & Rocha, E. P. C. Pervasive domestication of defective prophages by
591 bacteria. *Proc. Natl. Acad. Sci.* **111**, 12127–12132 (2014).
592 13. Kageyama, M., Ikeda, K. & Egami, F. Studies of a Pyocin: III. Biological Properties of the Pyocin. *J.*
593 *Biochem. (Tokyo)* **55**, 59–64 (1964).
594 14. Heo, Y.-J., Chung, I.-Y., Choi, K. B. & Cho, Y.-H. R-type pyocin is required for competitive growth
595 advantage between Pseudomonas aeruginosa strains. *J. Microbiol. Biotechnol.* **17**, 180–185 (2007).
596 15. Ge, P. *et al.* Action of a minimal contractile bactericidal nanomachine. *Nature* **580**, 658–662 (2020).
597 16. Carim, S. *et al.* Systematic discovery of pseudomonad genetic factors involved in sensitivity to
598 tailocins. *ISME J.* **15**, 2289–2305 (2021).
599 17. Blasco, L. *et al.* Study of 32 new phage tail-like bacteriocins (pyocins) from a clinical collection of
600 *Pseudomonas aeruginosa* and of their potential use as typing markers and antimicrobial agents. *Sci.*
601 *Rep.* **13**, 117 (2023).
602 18. Saha, S. *et al.* F-Type Pyocins Are Diverse Noncontractile Phage Tail-Like Weapons for Killing
603 *Pseudomonas aeruginosa*. *J. Bacteriol.* **205**, e00029-23 (2023).
604 19. Zink, R., Loessner, M. J. & Scherer, S. Charaterization of cryptic prophages (monocins) in Listeria
605 and sequence analysis of a holin/endolysin gene. *Microbiology* **141**, 2577–2584 (1995).
606 20. Lee, G. *et al.* F-Type Bacteriocins of *Listeria monocytogenes*: a New Class of Phage Tail-Like
607 Structures Reveals Broad Parallel Coevolution between Tailed Bacteriophages and High-Molecular-
608 Weight Bacteriocins. *J. Bacteriol.* **198**, 2784–2793 (2016).
609 21. Sigal, N. *et al.* Specialized *Listeria monocytogenes* produce tailocins to provide a population-level
610 competitive growth advantage. *Nat. Microbiol.* **9**, 2727–2737 (2024).
611 22. Gu, Z., Ge, X. & Wang, J. Structure of an F-type phage tail-like bacteriocin from *Listeria*
612 *monocytogenes. Nat. Commun.* **16**, 1695 (2025).
613 23. Gebhart, D. *et al.* Novel High-Molecular-Weight, R-Type Bacteriocins of *Clostridium difficile*. *J.*
614 *Bacteriol.* **194**, 6240–6247 (2012).

615 24. Cai, X. *et al.* Atomic structures of a bacteriocin targeting Gram-positive bacteria. *Nat. Commun.* **15**,
616 7057 (2024).
617 25. Cheng, S. *et al.* Complete Genome Sequence of a New *Enterococcus faecalis* Bacteriophage,
618 vB_EfaS_IME197. *Genome Announc.* **4**, e00827-16 (2016).
619 26. Edgar, R. C. MUSCLE: multiple sequence alignment with high accuracy and high throughput.
620 *Nucleic Acids Res.* **32**, 1792–1797 (2004).
621 27. Afonina, I. *et al.* The composition and function of *Enterococcus faecalis* membrane vesicles.
622 *microLife* **2**, uqab002 (2021).
623 28. McBride, S. M., Fischetti, V. A., LeBlanc, D. J., Moellering, R. C. & Gilmore, M. S. Genetic
624 Diversity among Enterococcus faecalis. *PLoS ONE* **2**, e582 (2007).
625 29. Powell, H. R., Islam, S. A., David, A. & Sternberg, M. J. E. Phyre2.2: A Community Resource for
626 Template-based Protein Structure Prediction. *J. Mol. Biol.* **437**, 168960 (2025).
627 30. Dunne, M. *et al.* Reprogramming Bacteriophage Host Range through Structure-Guided Design of
628 Chimeric Receptor Binding Proteins. *Cell Rep.* **29**, 1336-1350.e4 (2019).
629 31. Abramson, J. *et al.* Accurate structure prediction of biomolecular interactions with AlphaFold 3.
630 *Nature* **630**, 493–500 (2024).
631 32. Spinelli, S., Veesler, D., Bebeacua, C. & Cambillau, C. Structures and host-adhesion mechanisms of
632 lactococcal siphophages. *Front. Microbiol.* **5**, (2014).
633 33. Ayala, R. *et al.* Nearly complete structure of bacteriophage DT57C reveals architecture of head-to-
634 tail interface and lateral tail fibers. *Nat. Commun.* **14**, 8205 (2023).
635 34. d'Acapito, A., Decombe, A., Arnaud, C.-A. & Breyton, C. Comparative anatomy of siphophage tails
636 before and after interaction with their receptor. *Curr. Opin. Struct. Biol.* **92**, 103045 (2025).
637 35. Xu, Y., Murray, B. E. & Weinstock, G. M. A Cluster of Genes Involved in Polysaccharide
638 Biosynthesis from *Enterococcus faecalis* OG1RF. *Infect. Immun.* **66**, 4313–4323 (1998).

639 36. Teng, F., Singh, K. V., Bourgogne, A., Zeng, J. & Murray, B. E. Further Characterization of the *epa*
640 Gene Cluster and Epa Polysaccharides of *Enterococcus faecalis*. *Infect. Immun.* **77**, 3759–3767
641 (2009).
642 37. Palmer, K. L. *et al.* Comparative Genomics of Enterococci: Variation in *Enterococcus faecalis*, Clade
643 Structure in E. faecium, and Defining Characteristics of *E. gallinarum* and *E. casseliflavus*. *mBio* **3**,
644 e00318-11 (2012).
645 38. Salamzade, R. *et al.* zol and fai: large-scale targeted detection and evolutionary investigation of gene
646 clusters. *Nucleic Acids Res.* **53**, gkaf045 (2025).
647 39. Clewell, D. B. *et al.* Mapping of *Streptococcus faecalis* plasmids pAD1 and pAD2 and studies
648 relating to transposition of Tn917. *J. Bacteriol.* **152**, 1220–1230 (1982).
649 40. Sharpe, M. E. Serological Types of *Streptococcus faecali*s and its Varieties and their Cell Wall Type
650 Antigen. *J. Gen. Microbiol.* **36**, 151–160 (1964).
651 41. Thurlow, L. R., Thomas, V. C. & Hancock, L. E. Capsular Polysaccharide Production in
652 *Enterococcus faecalis* and Contribution of CpsF to Capsule Serospecificity. *J. Bacteriol.* **191**, 6203–
653 6210 (2009).
654 42. Guerardel, Y. *et al.* Complete Structure of the Enterococcal Polysaccharide Antigen (EPA) of
655 Vancomycin-Resistant *Enterococcus faecalis* V583 Reveals that EPA Decorations Are Teichoic
656 Acids Covalently Linked to a Rhamnopolysaccharide Backbone. *mBio* **11**, e00277-20 (2020).
657 43. Davis, J. L. *et al.* Dissecting the Enterococcal Polysaccharide Antigen (EPA) structure to explore
658 innate immune evasion and phage specificity. *Carbohydr. Polym.* **347**, 122686 (2025).
659 44. Gilmore, M. S. & Haas, W. The selective advantage of microbial fratricide. *Proc. Natl. Acad. Sci.*
660 **102**, 8401–8402 (2005).
661 45. Chatterjee, A. *et al.* Bacteriophage Resistance Alters Antibiotic-Mediated Intestinal Expansion of
662 Enterococci. *Infect. Immun.* **87**, e00085-19 (2019).
663 46. Lebreton, F. *et al.* Emergence of Epidemic Multidrug-Resistant *Enterococcus faecium* from Animal
664 and Commensal Strains. *mBio* **4**, e00534-13 (2013).

665 47. Schloissnig, S. *et al.* Genomic variation landscape of the human gut microbiome. *Nature* **493**, 45–50
666 (2013).
667 48. Clewell, D. B. *et al.* Extrachromosomal and Mobile Elements in Enterococci: Transmission,
668 Maintenance, and Epidemiology. in *Enterococci: From Commensals to Leading Causes of Drug*
669 *Resistant Infection* (eds Gilmore, M. S., Clewell, D. B., Ike, Y. & Shankar, N.) (Massachusetts Eye
670 and Ear Infirmary, Boston, 2014).
671 49. Ghequire, M. G. K. & De Mot, R. The Tailocin Tale: Peeling off Phage Tails. *Trends Microbiol.* **23**,
672 587–590 (2015).
673 50. Krupovic, M. & Koonin, E. V. Multiple origins of viral capsid proteins from cellular ancestors. *Proc.*
674 *Natl. Acad. Sci.* **114**, (2017).
675 51. Sarris, P. F., Ladoukakis, E. D., Panopoulos, N. J. & Scoulica, E. V. A Phage Tail-Derived Element
676 with Wide Distribution among Both Prokaryotic Domains: A Comparative Genomic and
677 Phylogenetic Study. *Genome Biol. Evol.* **6**, 1739–1747 (2014).
678 52. Punjani, A., Rubinstein, J. L., Fleet, D. J. & Brubaker, M. A. cryoSPARC: algorithms for rapid
679 unsupervised cryo-EM structure determination. *Nat. Methods* **14**, 290–296 (2017).
680 53. Posit team (2025). RStudio: Integrated Development Environment for R. Posit Software, PBC,
681 Boston, MA.
682 54. Kutter, E. Phage Host Range and Efficiency of Plating. in *Bacteriophages* (eds Clokie, M. R. J. &
683 Kropinski, A. M.) vol. 501 141–149 (Humana Press, Totowa, NJ, 2009).
684 55. Carlson, K. *Working with Bacteriophages: Common Techniques and Methodological Approaches,*
685 *Vol 1. CRC Press, Boca Raton, FL.*
686 56. Broad Institute. Data from Bioproject PRJNA313452. NCBI Genbank.
687 57. Broad Institute. Data from Bioproject PRJNA663900. NCBI Genbank.
688 58. Mass Eye and Ear/ Harvard Medical School. NCBI Genbank. Data from Bioproject PRJNA1371623.
689 59. Li, H. & Durbin, R. Fast and accurate short read alignment with Burrows–Wheeler transform.
690 *Bioinformatics* **25**, 1754–1760 (2009).

691 60. Walker, B. J. *et al.* Pilon: An Integrated Tool for Comprehensive Microbial Variant Detection and
692 Genome Assembly Improvement. *PLoS ONE* **9**, e112963 (2014).
693 61. Darling, A. E. *et al.* PhyloSift: phylogenetic analysis of genomes and metagenomes. *PeerJ* **2**, e243
694 (2014).
695 62. Parks, D. H., Imelfort, M., Skennerton, C. T., Hugenholtz, P. & Tyson, G. W. CheckM: assessing the
696 quality of microbial genomes recovered from isolates, single cells, and metagenomes. *Genome Res.*
697 **25**, 1043–1055 (2015).
698 63. Jain, C., Rodriguez-R, L. M., Phillippy, A. M., Konstantinidis, K. T. & Aluru, S. High throughput
699 ANI analysis of 90K prokaryotic genomes reveals clear species boundaries. *Nat. Commun.* **9**, 5114
700 (2018).
701 64. Van Dijk, L. R. *et al.* StrainGE: a toolkit to track and characterize low-abundance strains in complex
702 microbial communities. *Genome Biol.* **23**, 74 (2022).
703 65. Arndt, D. *et al.* PHASTER: a better, faster version of the PHAST phage search tool. *Nucleic Acids*
704 *Res.* **44**, W16–W21 (2016).
705 66. Seemann, T. Prokka: rapid prokaryotic genome annotation. *Bioinformatics* **30**, 2068–2069 (2014).
706 67. Mistry, J. *et al.* Pfam: The protein families database in 2021. *Nucleic Acids Res.* **49**, D412–D419
707 (2021).
708 68. Kanehisa, M. KEGG: Kyoto Encyclopedia of Genes and Genomes. *Nucleic Acids Res.* **28**, 27–30
709 (2000).
710 69. Karp, P. D. *et al.* The BioCyc collection of microbial genomes and metabolic pathways. *Brief.*
711 *Bioinform.* **20**, 1085–1093 (2019).
712 70. Price, M. N. & Arkin, A. P. PaperBLAST: Text Mining Papers for Information about Homologs.
713 *mSystems* **2**, e00039-17 (2017).
714 71. Georgescu, C. H. *et al.* SynerClust: a highly scalable, synteny-aware orthologue clustering tool.
715 *Microb. Genomics* **4**, (2018).
716 72. Schrödinger, L. & DeLano, W. PyMOL. (2020).

717 73. Pedregosa, F. *et al.* Scikit-learn: Machine learning in Python. *Journal of Machine Learning Research*
718 **12**, 2825–2830 (2011).
719 74. Emms, D. M. & Kelly, S. OrthoFinder: phylogenetic orthology inference for comparative genomics.
720 *Genome Biol.* **20**, 238 (2019).
721 75. Katoh, K., Kuma, K., Toh, H. & Miyata, T. MAFFT version 5: improvement in accuracy of multiple
722 sequence alignment. 8.
723 76. Minh, B. Q. *et al.* IQ-TREE 2: New Models and Efficient Methods for Phylogenetic Inference in the
724 Genomic Era. *Mol. Biol. Evol.* **37**, 1530–1534 (2020).
725 77. Gilmore, S. M., Earl, A., Prichula, J., Manson, A, Richards, G., Karumidze, N. & Lebreton, F.
726 Compositions and methods for control of specific bacterial populations. US Patent WO2025054631,
727 filed September 10, 2023. https://patentscope.wipo.int/search/en/WO2025054631.
728 78. Lossouarn, J. *et al.* Enterococcus faecalis Countermeasures Defeat a Virulent Picovirinae
729 Bacteriophage. *Viruses* **11**, 48 (2019).
730

731 **ACKNOWLEDGMENTS**

732 We thank Nicki E. Watson and the Harvard Center for Nanoscale Systems for technical assistance with
733 TEM. This work was supported by NIH grant AI083214 (Harvard-wide Program on Antibiotic
734 Resistance) and was also funded in part with federal funds from the National Institute of Allergy and
735 Infectious Diseases, National Institutes of Health, Department of Health and Human Services, under grant
736 numbers U19AI110818 (Broad Institute) and F32AI179151 (J.T.S). Work in the Kaplan laboratory at
737 UChicago was supported by the National Institute of General Medical Sciences (R35GM157116 to M.K.)
738 and the Searle Scholars Program (to M.K.). We gratefully acknowledge the expert technical assistance
739 and support provided by Ryan Whipple and Jose T. Saavedra. The authors also thank members of the
740 Gilmore and Earl Labs for helpful discussions during the development of this project and preparation of
741 the manuscript.

742

743 **AUTHOR CONTRIBUTIONS**

744 M.S.G. conceived the study. M.S.G. and J.P. designed the overall experimental work and A.M.E. and
745 A.L.M. supported project development and provided guidance on both the computational analyses and the
746 biological aspects. A.L.M., J.T.S., G.R., and J.P. performed all the bioinformatic analyses. N.K.
747 conducted the initial detection of efagin activity, and the efagin deletion mutant in OG1RF was
748 constructed by N.K. and S.S.M. J.P. optimized efagin production and purification, performed activity
749 assays, and generated efagin-resistant mutants and efagin chimeras. A.C. and M.K. performed the efagin
750 particle measurements. J.P., A.L.M., J.T.S., A.M.E., and M.S.G. contributed to data interpretation and
751 scientific discussion. J.P. and M.S.G. wrote the original draft, and J.P., A.L.M., J.T.S., and M.S.G.
752 revised and edited the manuscript. A.M.E. and M.S.G. acquired funding and supervised the project. All
753 authors read and approved the final manuscript.

754

755 **DECLARATION OF INTERESTS**

756 M.S.G., A.M.E., J.P., A.L.M., G.R., and N.K. are listed as co-inventors on a patent application related to
757 efagin – WO2025054631 [https://patentscope.wipo.int/search/en/WO2025054631][77]. All other authors
758 declare no competing interests.

759

760 **ADDITIONAL RESOURCES**

761 All genomes used in this study are described in **Tables S1, S5, S7, S11, S24, and S25.**
762 Broad Institute. Data from Bioproject PRJNA313452. NCBI Genbank.
763 https://www.ncbi.nlm.nih.gov/bioproject/?term=PRJNA313452.

764 Broad Institute. Data from Bioproject PRJNA663900. NCBI Genbank.
765 https://www.ncbi.nlm.nih.gov/bioproject/?term=PRJNA663900.
766 Mass Eye and Ear/ Harvard Medical School. Data from Bioproject PRJNA1371623. NCBI Genbank.
767 https://dataview.ncbi.nlm.nih.gov/object/PRJNA1371623.
768

769 **EXTENDED DATA FIGURES**

770 **Extended Data Fig. 1. Genomic neighborhood of efagin shows conserved flanking genes**. Bar plots
771 display the frequency of genes found upstream (left) and downstream (right) of efagin across *E. faecalis*
772 genomes. The most common gene at each position is shown in red, the second in green, and the third in
773 purple.

774 **Extended Data Fig. 2. Comparison of gene clusters encoding phage tail-like elements.** Pyocin (30.3
775 kb), diffocin (21.8 kb), monocin (11.6 kb), and efagin (14.6 kb) from *Pseudomonas*
776 *aeruginosa*, *Clostridium difficile*, *Listeria monocytogenes*, and *Enterococcus faecalis*, respectively. While
777 these systems show broad similarity in gene organization, they share little to no sequence identity,
778 suggesting independent evolutionary origins. Genomic comparison between the *L.*
779 *monocytogenes* monocin locus and the *E. faecalis* efagin locus reveals similar gene organization,
780 particularly in structural modules such as the tube, tape measure, baseplate components, and receptor-
781 binding protein (RBP). Although efagin shares organizational similarity with monocin, it has minimal
782 sequence identity with monocin across three genes (red asterisk). Both systems encode non-contractile
783 phage tail-like structures and appear to have arisen independently. Arrows represent open reading frames
784 (ORFs), color-coded by predicted function: regulatory (lightly grey), structural (pink), and lysis-associated
785 genes (purple). Particles are classified as R-type (contractile) or F-type (non-contractile). Reference
786 sequences used include: i) the R- and F-type pyocin clusters from *Pseudomonas aeruginosa* PAO1,
787 corresponding to the genomic region spanning genes PA0610–PA0648 (Genbank: AE004091.2); ii) the R-
788 type diffocin from *Clostridium difficile* 630 (GenBank: NZ_CP010905.2; genes CD1359–CD1379); iii) the

789 F-type monocin from *Listeria monocytogenes* 10403S (GenBank: NC_017544.1; genes LMRG02361–
790 LMRG02378); and iv) efagin from *E. faecalis* V583 (GenBank: NC_004668.1; genes ef1276–ef1293)
791 were included as reference sequences. The number inside each arrow denotes the number of genes
792 represented.

793 **Extended Data Fig. 3. Distribution of contractile (R-type) and non-contractile (F-type) phage tail-like**
794 **elements among genomes from Gram-positive and Gram-negative bacterial species.** In contrast to
795 efagin, which is highly conserved and intact in all strains for which high-quality genome sequences are
796 available, the other tailocins appear variable and often occur in alternate hybrid forms.

797 **Extended Data Fig. 4. Predicted model for EF1291 as ribbon and space-filling structures using**
798 **Alphafold 3.**[31] The three colors (blue, red, and yellow) represent individual monomers within the trimer.
799 Regions highlighted with darker colors in the C-terminal end correspond to the EF1291 structural regions
800 related to the receptor-binding domain of Listeria phage PSA protein gp15 by Phyre2.2.[29]

801 **Extended Data Fig. 5. Coordinated variation of *epa* gene presence/absence and efagin-associated**
802 **SNPs across *E. faecalis* representative genomes.** Example of a correlation between a sequence variant
803 in efagin *ef*1291 and the presence or absence of a specific gene in the *epa,* across the diversity of *E. faecalis*
804 strains. This plot shows variation in position 12903 of *ef*1291 and the presence or absence of the *epa* gene
805 *ef*2167. Gray shading indicates presence or absence concordance between mutated position 12903 and
806 *ef*2167. Similar correlations were observed between efagin positions and *ef*2166, *ef*2167, *ef*2168, and
807 *ef*2169, four adjacent genes within the *epa*.

808 **Extended Data Fig. 6. Efagin resistant mutants have defects in *epa* variable region genes. a,** Effect
809 of *epa* mutations on efagin susceptibility in four *E. faecalis* strains (FA2-2, X98, V583, and OG1RF). **b,**
810 Other studies[43,45, 78] describing *epa* mutations or indels correlated with phage resistance

811

812 **Extended Data Fig. 7. Relationship between efagin activity and *epa* operon architecture across 54 *E.***
813 ***faecalis* strains.** Schematic figure showing the left-hand heat maps display efagin activity assays from five
814 different donor strain: OG1RF (type C efagin) and OG1RF chimeras: *χefgA* (type A efagin), *χefgB* (type B
815 efagin), *χefgD* (type D efagin), and *χefgE* (type E efagin), annotated with its *epa* operon type and assigned
816 efagin type (A-E) against a diverse collection of *E. faecalis* strains (n=54). Grey indicates susceptible and
817 white non-susceptibility. Grey hashing highlights donor–target pairs that share either the same efagin
818 (hashes pointing up to the right) or/ and *epa* type (hashes pointing up to the left), indicating situations where
819 we would not expect inhibition, and most often do not observe inhibition (**Table S19**). Operon cluster IDs
820 are listed for each target strain. The figure highlights how variations in *epa* gene content, and efagin type
821 are associated with differential killing profiles. Chimeric constructs are denoted using the Greek letter "χ"
822 (chi), and efagin is abbreviated as "*efg*."

823 **Extended Data Fig. 8. Comparison of the organization of the *epa* locus between *E. faecalis* V583 and**
824 ***E. faecium* Aus0004.** The *epa* rhamnose backbone is conserved in both species (dark yellow arrows), but
825 differs in gene composition and arrangement, whereas the variable region (light yellow arrows) is
826 completely different in the two species. Core *epa* genes (*epa*A–*epa*R) show moderate to high sequence
827 identity (31.2–92.1%), whereas the variable decoration genes (light yellow) lack detectable homology,
828 highlighting species-specific diversification of surface polysaccharide structures. In *E. faecium*, the locus
829 follows the order *epa*ABCDEFGHPQLMNOR. The *E. faecium epa*N gene resembles *E. faecalis epa*N at
830 the N-terminus, sharing a predicted S-adenosylmethionine binding site, but differs in its C-terminal
831 sequence. We identified orthologs of *epa*P and *epa*Q in both species, but located at distinct genomic sites.
832 In *E. faecalis*, the central region of the cluster contains *epa*I, *epa*J, and *epa*K, whereas in *E. faecium* these
833 genes are absent and replaced by *epa*P and *epa*Q, suggesting the rhamnose polysaccharides of the two
834 species have different structure.

835 **Extended Data Fig. 9. Structural diversity of *epa* operons across *E. faecium* strains and correlation**
836 **with efagin susceptibility**. Strain identifier, sequence type (ST), clonal complex (CC), *E. faecium* clade

assignments (A1, A2, or B) and vancomycin resistance genotype in relation to the organization of *epa* operons. Rec indicates strains that are hybrids between clades. Conserved core genes are shown in black, while variable genes are colored according to orthogroup membership, with shapes corresponding to predicted function. The rightmost panel shows the efagin susceptibility profile. In the Epa cluster, black represents core genes found in all the genomes, and grey indicates rare genes found in less than 5%.

Extended Data Fig. 10. Conservation of *epa* operon genes across *Enterococcus* species and correlation with efagin susceptibility. Strains of *Enterococcus* clades are colored in graded shades of purple by membership in clades I – IV.[1] The extent of amino acid sequence identity with inferred *Epa* gene products, when compared to the prototypes of *E. faecalis* strain V583, is indicated by the gold heatmap. Efagin susceptibility is indicated with grey shading.

SUPPLEMENTARY FIGURES

Supplementary Fig. 1. V583 efagin gene function prediction. Biocyc, PaperBlast, Phyre2.2, Blastp, Prokka, Pfam, and Alphafold were used to infer the function.

Supplementary Fig. 2. Variation of *epa* gene presence/absence and efagin-associated SNPs across *E. faecalis* representative genomes. This plot shows the distribution of *epa* gene presence (yellow) and efagin *ef*1291 SNPs (red) across *E. faecalis* strains, aligned to a whole-genome phylogeny (center). Concordance between these *ef*1291 SNPs and the presence of these specific *epa* genes was observed in 81% of strains, far exceeding the ~50% expected by chance, suggesting coordinated evolutionary dynamics. The enrichment of these reciprocal patterns supports a functional or selective relationship between efagin and the *epa* locus.

Supplementary Fig. 3. Visualization of efagin from OG1RF*χefgD* chimera strain. Transmission electron microscopy (TEM) shows images of efagin particles produced by the *E. faecalis* OG1RF*χefgD*

860 chimera strain expressing type D efagin. Morphological features were visualized and quantified using TEM
861 and analyzed with Fiji/ImageJ software.

862 **Supplementary Fig. 4. Gene structure of representatives of *Epa* type 11 in 10 *E. faecalis* genomes**.
863 Each row represents a distinct *E. faecalis* genome, labeled by its NCBI accession number. Conserved
864 core *epa* genes are shown in black, while variable genes (e.g., 000192, 000190, etc.) are represented in
865 distinct colors, highlighting differences in the epa operon across strains, within *Epa* type 11.

866 **Supplementary Fig. 5. Frequency of combinations of efagin and EPA types present in 493 *E. faecalis***
867 **representative genomes.** Rows represent different efagin types; columns represent different *epa* types. The
868 central heat map indicates the frequency of each combination of *epa* and efagin types; marginal bar plots
869 show the frequency of each *epa* or efagin type individually across the 493 genomes. A white square
870 indicates that there are no genomes with that combination of efagin and *epa* types.

871 **Supplementary Fig. 6. Whole-genome phylogeny of *E. faecalis* strains, overlaid with the diversity of**
872 ***epa* types (outer ring; 1-20) and efagin types (inner ring; A-E, and X).** The lack of concordance between
873 the genomic phylogeny and the distribution of efagin or epa types suggests that efagin and *epa* genetic
874 diversity were likely acquired by horizontal gene transfer and localized recombination. Scale bar indicates
875 genetic distance.

876

877 **SUPPLEMENTARY TABLES**

878 **Table S1.** BLAST results of efagin against 3,068 high-quality *E. faecalis* genomes
879 **Table S2.** Summary of Genomad-identified phage-derived elements in *Melissococcus plutonius*
880 **Table S3.** Summary of Phastest-identified phage-derived elements in *Melissococcus plutonius*
881 **Table S4.** Results of BLAST analysis comparing efagin and monocin
882 **Table S5.** Summary of monocin loci identified in 74 *Listeria monocytogenes* genomes

883 **Table S6.** Monocin deletion identified across 13 *Listeria monocytogenes* genomes

884 **Table S7.** Summary of R-type pyocin loci detected across 343 *Pseudomonas aeruginosa* genomes

885 **Table S8**. R-pyocin variant region identified across 187 *Pseudomonas aeruginosa* genomes

886 **Table S9.** Summary of F-type pyocin loci detected across 343 *Pseudomonas aeruginosa* genomes

887 **Table S10.** F-pyocin variant region identified across 55 *Pseudomonas aeruginosa* genomes

888 **Table S11.** Summary of R-type diffocin loci detected across 32 *Clostridium difficile* genomes

889 **Table S12.** R-diffocin variant region identified across 18 *Clostridium difficile* genomes

890 **Table S13.** BLAST results for the *E. faecalis* phage most closely related to the efagin

891 **Table S14.** List of efagin and *epa* types assigned to 1,972 *E. faecalis* genomes included in the study

892 **Table S15.** BLAST results of type E efagin C-terminal end

893 **Table S16.** V583 efagin gene function prediction performed by Prokka, Pfam, and KEGG

894 **Table S17.** Whole-genome sequencing data of spontaneous efagin-resistant *E. faecalis* mutants

895 **Table S18.** EPA orthogroup dataset of 1,972 *E. faecalis* genomes

896 **Table S19.** Statistical analysis of the association between efagin or *epa* type matching and susceptibility to

897 killing

898 **Table S20.** EPA orthogroup dataset of 58 *E. faecium* genomes

899 **Table S21.** Amino acid identity between epa core genes of *E. faecalis* V583 and *E. faecium* Aus0004 based

900 on BLASTP alignments

901 **Table S22.** Amino acid sequence identity (%) between genes from the epa cluster of *E. faecalis* V583, and

902 their top hit in 40 *Enterococcus* species

903 **Table S23.** List of *E. faecalis* strains used in the experimental work

904 **Table S24.** List of *E. faecium* strains used in the experimental work

905 **Table S25.** List of *Enterococcus* species used in the experimental work

906 **Table S26.** List of strains used in this study

907 **Table S27.** List of primers used in this study